Laser and Particle Beams (2014), *32*, 15–20.

doi:10.1017/S0263034613000797

Time-of-flight spectra for mapping of charge density of ions produced by laser

J. KRÁSA,[1] P. PARYS,[2] L. VELARDI,[3,4] A. VELYHAN,[1] L. RYĆ,[2] D. DELLE SIDE,[3,4] AND V. NASSISI[3,4]

[1]Institute of Physics, ASCR, Prague, Czech Republic
[2]Institute of Plasma Physics and Laser Microfusion, Warsaw, Poland
[3]LEAS, Dipartimento di Matematica e Fisica, Università del Salento, Lecce, Italy
[4]INFN Sezione di Lecce, Lecce, Italy

(Received 16 July 2013; Accepted 21 August 2013)

Abstract

A space-resolved charge density of ions is derived from a time-resolved current of ions emitted from laser-produced plasma and expanded into the vacuum along collision-free and field-free paths. This derivation is based on a similarity relationship for ion currents with "frozen" charges observed at different distances from the target. This relationship makes it possible to determine a map of ion charge density at selected times after the laser plasma interaction from signals of time-of-flight detectors positioned at a certain distance from the target around a target-surface normal. In this work, we present maps of the charge density of ions emitted from Cu and polyethylene plasmas. The mapping demonstrates that bursts of ions are emitted at various ejection angles ϕ_n with respect to the target-surface normal. There are two basic directions ϕ_1 and ϕ_2, one belonging to the fastest ions, i.e., protons and carbon ions, and the other one to the slowest ions being a part of each plasma plume.

Keywords: Angular distribution of slow and fast ions; Ion expansion; Laser ion sources; Map of ion charge density; Modeling

INTRODUCTION

Laser ion sources are devices delivering ion beams useful for material modification as well as for basic particle emission physics (Dubenkov *et al.*, 1996; Haseroth & Hora, 1996). Transport of the extracted ion beam is affected by free expansion of the generated plasma into the vacuum which can be visualized by mapping the positions of ions. In this paper, we propose a method of visualization, which we call mapping of charge density of laser-produced ions. For investigation of laser-produced plasma as a source of ions, the diagnostics based on the time-of-flight (TOF) method is mainly applied. In order to determine space properties of expanding plasma, a number of ion detectors located at various angles ϕ with respect to the target surface normal or to the laser vector are employed.

The general trend in the angular distribution of emitted ions has been determined by an expression of a two-component structure (Thum *et al.*, 1994; Thum-Jäger & Rohr, 1999):

$$S(\phi) = a\cos(\phi - \phi_o) - b\cos^n(\phi - \phi_o), \quad (1)$$

where $S(\phi)$ is the density of particles in the zenithal direction, ϕ, and ϕ_0 denotes the declination (ejection angle) from the target surface normal direction caused by the laser-plasma interaction (Thum *et al.*, 1994); usually ϕ_0 differs from the impact angle of the laser beam ϕ_L.

The proposed technique of angular distribution mapping of the ion emission from laser-produced plasma is based on the analysis and computing signals of TOF ion collectors (IC) positioned at various angles ϕ_{IC}. All the ion collectors should be positioned far from the target where the charge states are already stable because the three-body recombination does not significantly affect the evolution of the expanding plasma lowering the charge state of ions any more. On the basis of this model, the plasma charge states can be assumed to be frozen at the distance of several tens of centimeters from the target (L_{cr}) (Roudskoy, 1996; Thum-Jäger & Rohr, 1999; Krása *et al.*, 1999; Lorusso *et al.*, 2005).

Address correspondence and reprint requests to: J. Krása, Institute of Physics, ASCR, v.v.i.Na Slovance 2, 182 21 Praha 8, Czech Republic. E-mail: krasa@fzu.cz

The creation of an ion map means transforming time-resolved ion currents, i.e., TOF spectra, observed in various directions into both angular and distance dependent distributions of the ion charge density. The aim of our work is to apply the innovated distance-of-flight diagnostic which offers the advantages of mapping the space distribution of ion charge density with the use of data from a number of TOF ion collectors. This mapping reveals more details on the ion emission from laser ion sources than the set of data from the TOF collectors.

THEORY

The signal $S_x(t)$ of a TOF ion collector measuring the current of impacted ions in x-direction depends on its response to ions' number and velocity given by a three-dimensional velocity distribution function $f(\vec{v})$ (Kelly & Dreyfus, 1988; Miotello & Kelly, 1999):

$$S_x(L, t) \propto v_x f(\vec{v})\, d\vec{v}. \tag{2}$$

To obtain the number of ions hitting the ion detector's area $dS = dydz$ per dt at a distance L from the target, the right side of (2) has to be transformed into laboratory space and time: $dv_x dv_y dv_z = (L/t^4)dSdt$. Substituting L/t for v and multiplying (2) by the charge eq carried by ions (where e is the elementary charge and q is the ion charge-state), one gets the signal function $S_x(L,t)$ of IC induced by the current of ions j_{IC} (Kelly & Dreyfus, 1988; Miotello & Kelly, 1999; Krása, 2013), which is represented by a voltage pulse $U_{IC}(L,t) = R\,S\,j_{IC}(L,t)$:

$$U_{IC}(L,t) = RS\kappa_0 L^2\, t^{-5} f(L/t), \tag{3}$$

where R is the load resistance, S the active IC area, and κ_0 is the normalizing coefficient of the product $L^2 t^{-5} f(L/t)$.

If the charge states of expanding ions have been frozen beyond a critical distance from the target, L_{cr}, where the three-body recombination becomes insignificant due to the plasma rarefaction (Roudskoy, 1996; Lorusso *et al.*, 2005), their total charge Q_0 can be regarded as constant, and we can derive the essential similarity relationship for ion currents detected by identical ion collectors which are placed at two different distances L_1 and L_2 in the same direction. Taking into consideration that the time-of-flight varies with the distance as $t = L/v$, Eq. (3) takes a form:

$$j(L,t)L^3 = \kappa_0 v^5 f(v), \tag{4}$$

and the similarity relationship for ion currents with "frozen" charges that are detected at different distances is

$$j(L_1, t_1)L_1^3 = j(L_2, t_2)L_2^3, \tag{5}$$

where $L_1/t_1 = L_2/t_2$.

The similarity relationship (5) enables us to determine the charge density distribution $q(x,\tau)$ over a distance-of-flight x at a selected time τ after the laser-matter interaction by the use of equation $q = j/v$, where the time-resolved current $j(L,t)$ is transformed to $q(x,\tau)$ applying the relationship between the flight times t, τ and the flight distances L, x as $L/t = x/\tau$. Consequently, dividing both sides of Eq. (5) by $v = L_1/t_1$ and substituting x, τ, L, t for L_1, t_1, L_2, t_2, respectively, we obtain the flight-distance dependence of the ion charge density, i.e., the distance-of-flight (DOF) spectrum, which at a time τ takes a form:

$$q(x, \tau) = j(x)\tau L^3/x^4. \tag{6}$$

The relationship (6) gives the transformation of the ion current density $j(L,t)$ in A/cm^2 to the ion charge density $q(x,\tau)$ in C/cm^3 at an arbitrary chosen instant τ after the laser-target interaction if the flight-time is replaced with the flight-distance making the substitution $x = L\tau/t$. A set of time-resolved ion currents recorded with the use of a number of ion collectors positioned in various directions with respect to the target surface normal allows us to obtain a set of ion charge densities $q_n(x,\tau)$ in these directions of observation. This set of DOF spectra $q_n(x,\tau)$ is the basis for creating ion-charge density maps $q_n(x, y, \tau)$ for any instant τ after the impact of the laser beam on the target.

When the detector is sensitive only to the charge of ions, relationship (2) takes a form $q(L,t)\ L^3 = \kappa_0\ v^4\ f(v)$. Then we get another significant relationship

$$q(L_1, t_1)L_1^3 = q(L_2, t_2)L_2^3, \tag{7}$$

where $L_1/t_1 = L_2/t_2$. For the total charge we get a well-known equation $q(L_1)L_1^2 = q(L_2)L_2^2$. This similarity relationship gives a simple and exact determination of the critical distance L_{cr} indicating that charge states of expanding ions have been "frozen" (Lorusso *et al.*, 2005).

EXPERIMENTAL ARRANGEMENT

The reported measurements were performed with iodine photodissociation laser systems at the PALS facility, Prague delivering onto a target a focused intensity of up to 3×10^{16} W/cm^2 in 300-ps pulses with $\lambda = 1.315$ μm and with a Compex 205 KrF excimer laser ($\lambda = 248$ nm, $\tau_{FWHM} = 23$ ns) at LEAS, Lecce which works at laser irradiances between 10^8 and 10^{10} W/cm^2. In these experiments, the TOF spectra of ions were measured at PALS by eight ion collectors and at LEAS by nine ion collectors positioned in a horizontal plane at various angles to the laser beam axis, as Figure 1 shows.

EXPERIMENTAL RESULTS AND DISCUSSION

The plasma produced at low irradiances of about 10^9 W cm^{-2} emits reproducible and smooth peak-shaped

https://doi.org/10.1017/S0263034613000797 Published online by Cambridge University Press

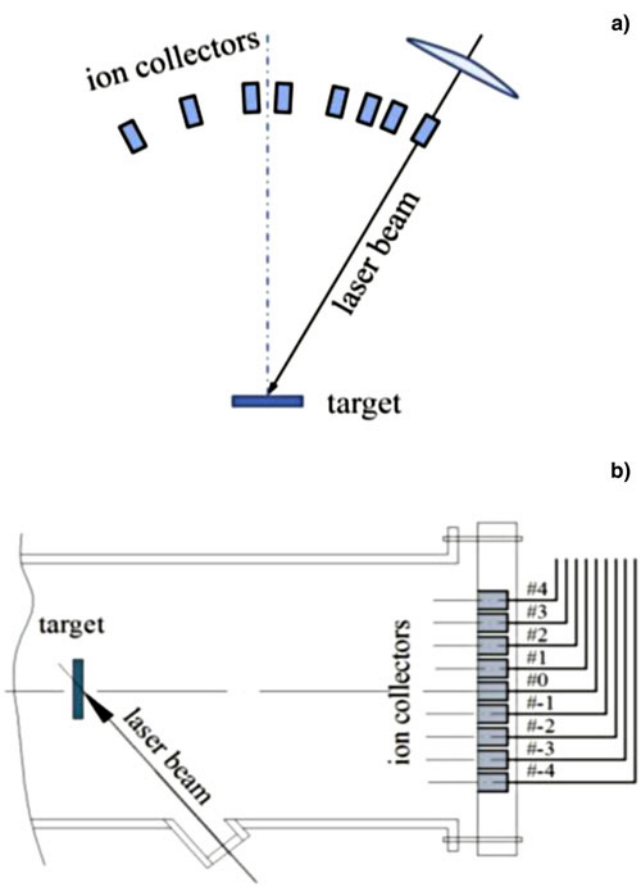

Fig. 1. (Color online) Schematic diagram of the experimental set-up of the iodine laser system PLAS (**a**) and of the KrF excimer laser at LEAS laboratory (**b**).

ion currents nearly free of shot-to-shot irregularities contrary to the plasma generated at higher intensities (10^{16} W cm^{-2}) (Krása *et al.*, 2009; 2011). Figure 2 shows such a reproducible emission of ions produced with a KrF excimer laser delivering 8-J/cm^2 fluence onto a Cu target. These nine time-resolved ion currents were observed at angles ranging from −19.5° to 19.5° with respect to the target surface normal at 0° in a clockwise direction. The laser pulse struck the target at 70°. The angular distribution is affected by the narrow angular distribution of ions having the highest charge states (Thum-Jäger & Rohr, 1999; Krása *et al.*, 2009). The width of the stream of ions, in fact, increases with decreasing ion charge-state.

If the charge of freely expanding ions is frozen, then the ion charge densities derived from TOF spectrum show variations over the axis of observation, as Figure 3 shows for different times $\tau = 5$ μs and 20 μs. Remarkable is the fast decrease in the ion charge density over a short distance of 20 cm from the target at 5 μs after the laser shot. The highest charge density at about 3 cm from the target belongs to the slowest ions while the fastest ions, i.e., protons and carbon ions, constituting the peak at 1.3 μs in Figure 2 became very rarefied up to a value of about 5×10^{-13} C/cm^3 at DOF = 33 cm, as the solid line in Figure 3 shows. The dash line in Figure 3 shows that the rarefaction caused by the ion expansion decreases the charge density significantly.

Unlike commonly presented angular distributions of the total number of emitted particles, total charge of ions, as well as a peak current, the transformation based on the relationship (6) makes it possible to map the charge density of ions over a plane of ion-current observation at selected instants, as Figure 4 shows. In this case, nine TOF spectra were transformed into DOF spectra and the map of ion charge density was created. Unfortunately, the space limitations inside the target chamber do not make it possible to put more ion collectors to obtain a fuller angular distribution of expanding ions. Figure 4 gives clear evidence that the space-distribution of ion charge density depends on the velocity of ions, i.e., on their acceleration mechanisms — the fastest ions (protons and carbon ions) carry the charge into the direction of an ion collector labeled with 9, i.e., angle of 19° (or higher),

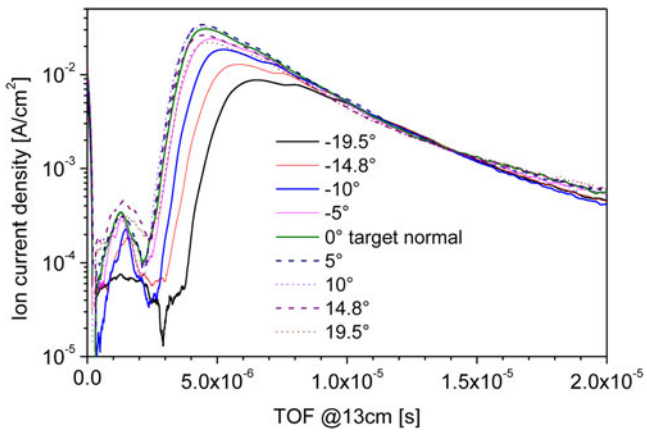

Fig. 2. (Color online) Time-of-flight spectra of Cu ions generated with the KrF excimer laser fluence of 8 J/cm^2. The laser beam struck the target at an angle of 70° with respect to the target surface normal.

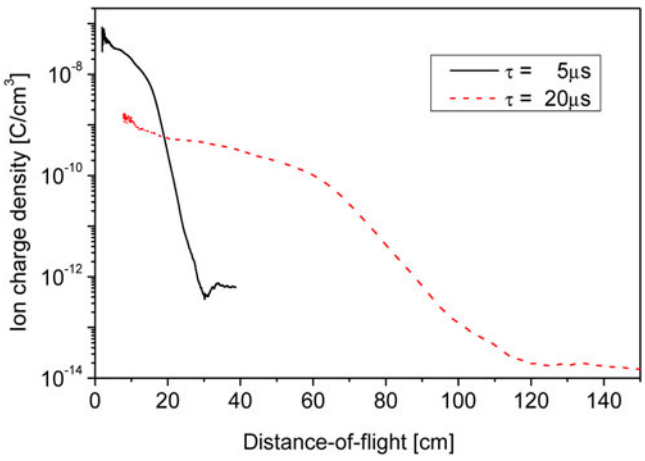

Fig. 3. (Color online) Ion charge density (DOF spectra) of Cu ions along the target surface normal, which were determined from TOF spectrum (see Fig. 2) with the use of Eq. (6) for selected times of 5 and 20 μs after the laser shot.

https://doi.org/10.1017/S0263034613000797 Published online by Cambridge University Press

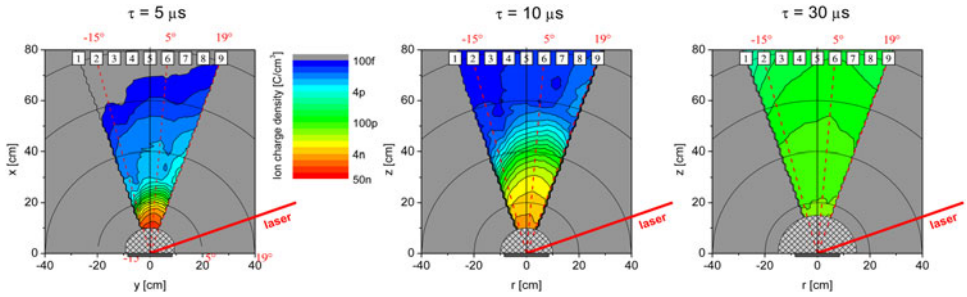

Fig. 4. (Color online) Charge density maps of ions emitted by Cu plasma at times of 5 μs, 10 μs and 30 μs after the laser-target interaction. These distributions were derived from TOF spectra shown in Figure 2. The labels indicate the directions of observation of ion currents with the use of the individual ion collectors positioned at the distance of 13 cm from the target surface. The KrF laser beam struck the target at an angle of 70° with respect to the target surface normal.

other local maxima of fast ions move in directions of −15° and 5° (see the dark-blue area in the map for $\tau = 5$ μs). The angle of expansion of slower Cu ions is well observable at later time of 30 μs as Figure 4 shows for $x < 30$ cm: $\phi \approx 8°$ (between ion collectors labeled 6 and 7).

A target irradiated by a medium laser-intensity can emit a high current of ions as Figure 5 shows for a polyethylene target exposed to intensity of 3×10^{16} W/cm^2. The ion current density reached a peak value of 37 A/cm^2 at a 40-cm distance from the target.

The velocity of fastest ions was higher than 2×10^9 cm/s, as can be determined from the DOF spectrum at the time of 400 ns in Figure 5b. This DOF spectrum shows that at the time $\tau = 400$ ns the rarefaction of ions transforms nearly all local peaks in the time-resolved current into inflection points on the DOF spectrum due to the term x^4 in (6). Owing to the high spread in velocity of ions the difference between the highest charge density and the lowest one is more than 7 orders of magnitude.

Figure 6 shows two maps of charge density at times of 400 and 820 ns after the laser pulse irradiation with the $(CH_2)_n$ target. It is obvious that the choice of the visualization time τ of the ion charge density allows us to highlight the variation in partial ejection angles of ion emission. The ion charge density map formed at $\tau = 400$ ns shows that the fastest ions are ejected in directions at −3° and 30° with respect to the target normal, while the map formed later at $\tau = 820$ ns shows that the slower ions expand at four ejection angles at −19°, 3°, 19°, and 30°. Thus, one can conclude that ions are emitted into various particular directions which are not fixed for all ion groups generated by the same laser pulse. Since the slower ions expand wider than the fast ones, it is possible to deduce that ions are accelerated by various mechanisms. Moreover, we can presume that the plasma expands in a form of a multi-jet fountain where the central jet is declined from the target surface normal and the others exhibit a high declination from this normal. Therefore, the simple angular distribution of emitted ions stated by the expression (1) for a two-component structure is not sufficient due to its time-integral conception that obliterates partial effects related to the minority groups of ionized species.

The ion charge density map, as a two-dimensional graph of the intensities, enables to display profiles of the charge density along a selected line parallel to the y-axis at various distances x from the target surface. Figure 7 shows line-profiles of the ion charge density at distances of 30, 50,

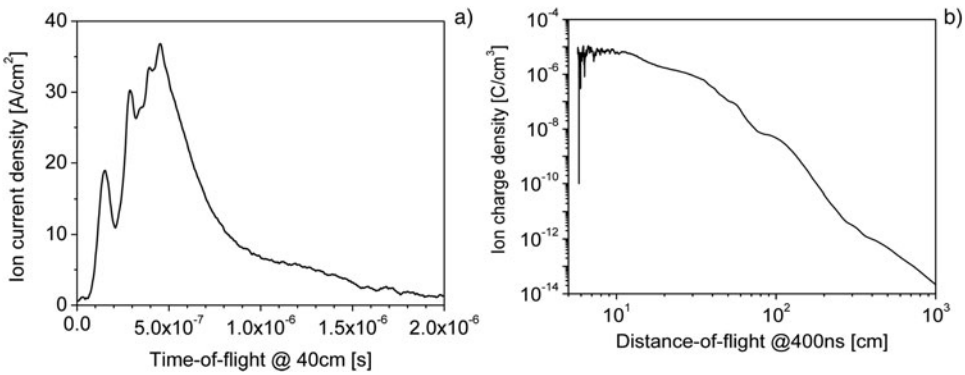

Fig. 5. Time-of-flight dependence of current density (**a**) and distance-of-flight dependence of charge density (**b**) of ions emitted from polyethylene plasma produced by intensity of 3×10^{16} W/cm^2. The iodine photo-dissociation laser beam struck the target at an angle of 30°. The ion collector was located at a distance of 40 cm from the target at an angle of −3° with respect to the target surface normal (label 3 in Fig. 6).

https://doi.org/10.1017/S0263034613000797 Published online by Cambridge University Press

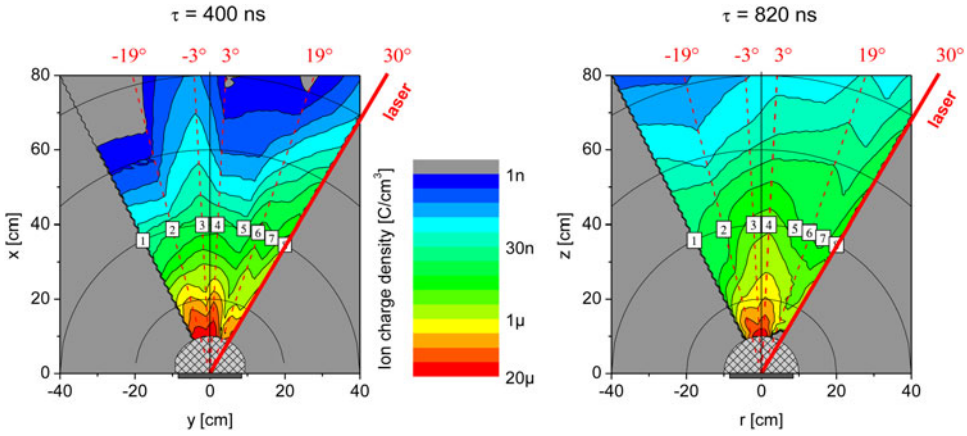

Fig. 6. (Color online) Charge density maps of protons and carbon ions at instants of 400 ns and 820 ns after the interaction of a PALS-laser beam with a $(CH_2)_n$ target. The labels indicate the directions of observation of ion currents with the use of eight ion collectors positioned at the distance of 40 cm from the target. The iodine photodissociation laser beam struck the target at the angle of 30°; target irradiation of 3×10^{16} W/cm^2.

and 80 cm from the Cu target surface at 20 μs after the laser-plasma interaction. Figure 8 shows the profiles of the ion charge density at 30, 50, and 70 cm far from the $(CH_2)_n$ target surface at time of 800 ns. These profiles also prove significant variations in the charge density of ions with increasing distance from the target at a selected time τ. In fact, these profiles match ions moving with different velocities given by the ratio x/τ. A similar state was described above for the CH_2 plasma produced by much higher laser intensity. Figure 8 also shows that the partial charge density profiles do not give a complete picture of the ion expansion because these profiles selected for flight-distances of 30, 50, and 70 cm at $\tau = 800$ ns show only four streams: 3 visible maxima and 1 assumed at $\phi_0 = 30^\circ$, while the total number of declinations ϕ_n is $n = 5$. Nevertheless, the line profiles shown in

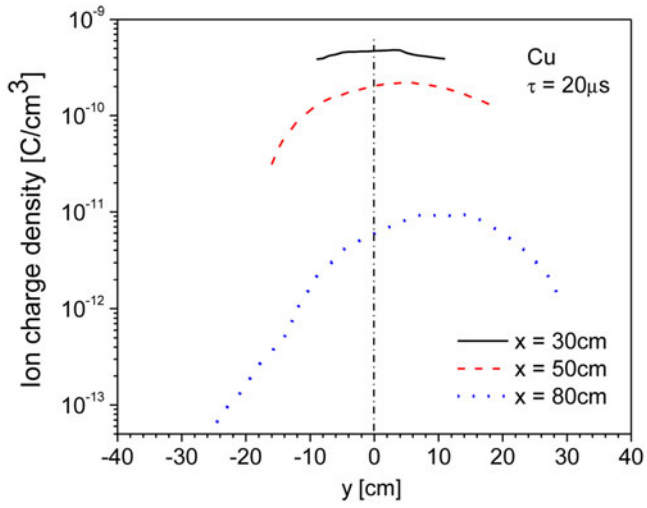

Fig. 7. (Color online) Line-profiles of the ion charge density along selected lines parallel to the *y*-axis at distances of 30, 50, and 80 cm from the Cu target surface at 20 μs after the laser-plasma interaction which were obtained from the charge density map shown in Figure 4.

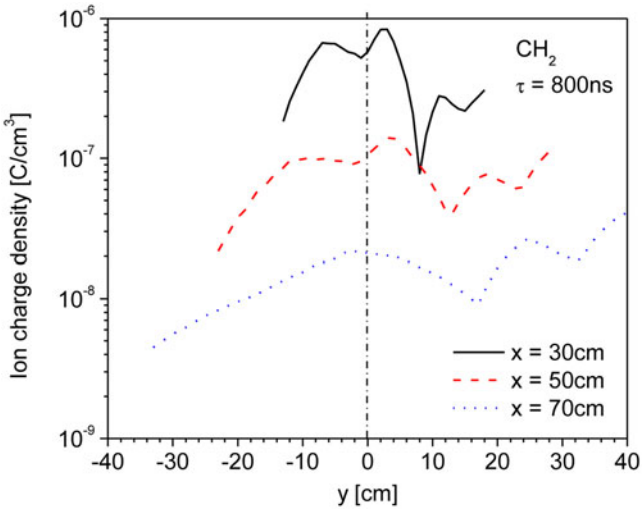

Fig. 8. (Color online) Line-profiles of the ion charge density along selected lines parallel to the *y*-axis at distances of 30, 50, and 70 cm from the $(CH_2)_n$ target surface at 800 ns after the laser-plasma interaction which were obtained from the charge density map shown in Figure 6.

Figures 7 and 8 enable us to compare the densities of expanding ions which were produced under different conditions.

CONCLUSIONS

In conclusion, these results confirm the usefulness of the concept of using the transformation of time-resolved ion currents (TOF spectra) to ion charge density profiles of ions (DOF spectra) over the direction of observation at a selected time τ after the laser-target interaction. The simultaneous measurement of TOF spectra of ions in various directions allows us to determine the map of the ion charge density at selected times. A set of these maps for various τ makes the visualization of the time development in the emission of ions possible if the charge of ions is frozen.

https://doi.org/10.1017/S0263034613000797 Published online by Cambridge University Press

The observed ion charge density maps show that the simple scenario of the plasma expansion, which is based on the idea that all groups of ionized species have the same declination ϕ_0 from the target surface normal, should be replaced by a new one reflecting the fact that ions are ejected into various angles ϕ_n in the dependence on their velocities. This multi-directionality in the ion emission appears even at low laser intensities which remains commonly undetected due to the averaging of the charge density over the ion velocity.

ACKNOWLEDGEMENTS

The authors gratefully acknowledge the support of the staff of the PALS laser facility which is a joint research laboratory of the Institute of Physics and the Institute of Plasma Physics of the Academy of Sciences of the Czech Republic without whose assistance this work would not have been possible. The research leading to these results has received funding from the Czech Science Foundation (Grant Nos. P205/12/0454), the Czech Republic's Ministry of Education, Youth and Sports (grant for the PALS RI - Project IC: LM2010014, and for the OPVK 3: CZ.1.07/2.3.00/20.0279), and from the LASERLAB-EUROPE (grant agreement n° 284464, EC's Seventh Framework Programme).

REFERENCES

Dubenkov, V., Sharkov, B., Golubev, A., Shumshurov, A., Shamaev, O., Roudskoy, I., Streltsov, A., Satov, Y., Makarov, K., Smakovsky, Y., Hoffmann, D., Laux, W., Müller, R.W., Spädtke, P., Stöckl, C., Wolf, B. & Jacoby, J. (1996). Acceleration of Ta^{10+} ions produced by laser ion source in RFQ MAXILAC, *Laser Part. Beams* **14**, 385–392.

Haseroth, H. & Hora, H. (1996). Physical mechanisms leading to high currents of highly charged ions in laser-driven ion sources, *Laser Part. Beams* **14**, 393–438.

Kelly, R. & Dreyfus, R.W. (1988). On the effect of Knudsen-layer formation on studies of vaporization, sputtering, and desorption. *Surf. Sci.* **198**, 263–276.

Krása, J., Láska, L., Rohlena, K., Pfeifer, M., Skála, J., Králiková, B., Straka, P., Woryna, E. & Wolowski, J. (1999). The effect of laser-produced plasma expansion on the ion population. *Appl. Phys. Lett.* **75**, 2539–2541.

Krása, J., Velyhan, A., Jungwirth, K., Krouský, E., Láska, L., Rohlena, K., Pfeifer, M. & Ullschmied, J. (2009). Repetitive outbursts of fast carbon and fluorine ions from sub-nanosecond laser-produced plasma. *Laser Part. Beams* **27**, 171–178.

Krása, J., Lorusso, A., Nassisi, V., Velardi, L. & Velyhan, A. (2011). Revealing of hydrodynamic and electrostatic factors in the center-of-mass velocity of an expanding plasma generated by pulsed laser ablation. *Laser Part. Beams* **29**, 113–119.

Krása, J. (2013). Gaussian energy distribution of fast ions emitted by laser-produced plasmas. *Appl. Surf. Sci.* **272**, 45–49.

Lorusso, A., Krása, J., Rohlena, K., Nassisi, V., Belloni, F. & Doria, D. (2005). Charge losses in expanding plasma created by an XeCl laser. *Appl. Phys. Lett.* **86**, 081501.

Miotello, A. & Kelly, R. (1999). On the origin of the different velocity peaks of particles sputtered from surfaces by laser pulses or charged-particle beams. *Appl. Surf. Sci.* 138–139, 44–51.

Roudskoy, I.V. (1996). General features of highly charged ion generation in laser-produced plasmas. *Laser Part. Beams* **14**, 369–384.

Thum, A., Rupp, A. & Rohr, K. (1994). Two-component structure in the angular emission of a laser-produced Ta plasma. *J. Phys. D: Appl. Phys.* **27**, 1791–1794.

Thum-Jäger, A. & Rohr, K. (1999). Angular emission distributions of neutrals and ions in laser ablated particle beams. *J. Phys. D: Appl. Phys.* **32**, 2827–2831.